Published in final edited form as:
Neuroimage. 2009 July 1; 46(3): 633–641. doi:10.1016/j.neuroimage.2009.03.001.

3T MRI relaxometry detects T2 prolongation in the cerebral normal-appearing white matter in multiple sclerosis

Mohit Neema[1], **Daniel Goldberg-Zimring**[1,2], **Zachary D. Guss**[1], **Brian C. Healy**[1], **Charles R.G. Guttmann**[1,2], **Maria K. Houtchens**[1], **Howard L. Weiner**[1], **Mark A. Horsfield**[3], **David B. Hackney**[4], **David C. Alsop**[4], and **Rohit Bakshi**[1,2]

[1] Department of Neurology, Brigham and Women's Hospital, Laboratory for Neuroimaging Research, Partners MS Center, Harvard Medical School, Boston, MA, USA

[2] Department of Radiology, Brigham and Women's Hospital, Laboratory for Neuroimaging Research, Partners MS Center, Harvard Medical School, Boston, MA, USA

[3] Department of Cardiovascular Sciences, University of Leicester, Leicester, UK

[4] Department of Radiology, Beth Israel Deaconess Medical Center, Harvard Medical School; Boston, MA, USA

Abstract

MRI at 3 T has increased sensitivity in detecting overt multiple sclerosis (MS) brain lesions; a growing body of data suggests clinically relevant damage occurs in the normal-appearing white matter (NAWM). We tested a novel pulse sequence to determine whether 3 T MRI spin–spin relaxometry detected damage in NAWM of MS patients (n = 13) vs. age-matched normal controls [(NL) (n = 11)]. Baseline characteristics of the MS group were: age (mean ± SD) 42.5 ± 5.4 (range 33–51 years), disease duration 9.0 ± 6.4 (range 1–22 years), Expanded Disability Status Scale score 2.5 ± 1.7 (range 1–6.5). Brain MRI measures, obtained at 3 T, included global and regional NAWM transverse relaxation rate [R2 (= 1/T2)], derived from 3D fast spin-echo T2 prepared images, and global white matter volume fraction derived from SPGR images. The regional NAWM areas investigated were the frontal lobe, parietal lobe, and the genu and splenium of the corpus callosum. Mean NAWM R2 was lower (indicating T2 prolongation) in MS than NL in the whole brain (p = 0.00047), frontal NAWM (p = 0.00015), parietal NAWM (p = 0.0069) and callosal genu (p = 0.0019). Similarly, R2 histogram peak position was lower in NAWM in MS than NL in the whole brain (p = 0.019). However, the normalized WM volume fractions were similar in both MS and NL (p > 0.1). This pilot study suggests that a novel 3D fast spin-echo pulse sequence at 3 T, used to derive R2 relaxation maps, can detect tissue damage in the global and regional cerebral NAWM of MS patients that is missed by conventional lesion and atrophy measures. Such findings may represent demyelination, inflammation, glial proliferation and axonal loss.

Introduction

Magnetic resonance imaging (MRI) has played a pivotal role in the diagnosis and management of multiple sclerosis (MS) (Bakshi et al., 2008). In addition, MRI metrics have become key supportive outcome measures to explore drug efficacy in clinical trials (Bakshi et al, 2005). Conventional MRI measures have contributed to the understanding of MS pathophysiology at the macroscopic level. However, a considerable amount of evidence suggests that these

Correspondence: Mohit Neema, MD, Brigham & Women's Hospital, Harvard Medical School Laboratory for Neuroimaging Research, One Brookline Place, Suite 602, Brookline, MA 02445, USA, Tel: 617-732-6118, Fax: 617-732-6540, mneema@bwh.harvard.edu.

measures lack specificity to underlying pathology and fail to capture diffuse occult disease affecting the cerebral white and gray matter (Neema et al., 2007a). Various advanced quantitative MRI measures have been developed that are particularly useful in revealing occult diffuse damage in the brain and spinal cord, and may therefore help resolve the dissociation between conventional MRI findings and clinical status (Neema et al., 2007b). One such technique, mapping the transverse relaxation time through T2 relaxometry, has shown promise in its ability to detect structural changes in normal-appearing white matter (NAWM) that escape detection by conventional MRI lesion measures ([Neema et al., 2007a], [Barbosa et al., 1994], [Miller et al., 1989], [Armspach et al., 1991], [Grenier et al., 2002] and [Whittall et al., 2002]).

The recent availability of high-field strength scanners, i.e. 3 T and higher, has the potential to revolutionize the research and clinical care in MS (Bakshi et al., 2008). 3 T MRI improves signal-to-noise ratio (SNR), which may enhance the sensitivity and specificity in identifying the full extent of the disease process (Schick, 2005). Such scanners reveal MS lesions in the brain with greater sensitivity than do 1.5 T scanners ([Sicotte et al., 2003], [Wattjes et al., 2006] and [Bachmann et al., 2006]). T2 relaxometry at 3 T is just beginning to be applied to the study of the brain in MS. A recent study demonstrated myelin damage in NAWM in patients with MS using one component of the T2 relaxation curve, the short T2 component, at 3 T (Oh et al., 2007). In the present study, we used a novel pulse sequence at 3 T to determine whether MRI histogram-based T2 relaxometric analysis could detect T2 prolongation in the regional and global cerebral NAWM in patients with MS.

Methods

Subjects

Demographic and clinical characteristics of the subjects are summarized in Table 1. We identified 13 patients with MS from a consecutive sample being prospectively enrolled and monitored as part of the Comprehensive Longitudinal Investigation of MS at Brigham (CLIMB) study at the Partners MS Center, Brigham and Women's Hospital, Boston, MA. CLIMB is an ongoing prospective observational cohort study that began following patients in 2000 (Gauthier et al., 2006). Inclusion of patients with MS in the current study was based on the following criteria: 1) age 18–55; 2) baseline neurological examination, including Kurtzke Expanded Disability Status Scale (EDSS) (Kurtzke, 1983) and Timed 25-Foot Walk (T25FW) assessment, performed by an MS specialist neurologist at the Partners MS Center; 3) established MS diagnosis at baseline of either relapsing-remitting (RR), secondary progressive or primary progressive by the International Panel criteria (Polman et al., 2005); 4) no other major medical disorder; 5) no relapse or corticosteroid use in the 4 weeks prior to study entry to avoid transient confounding effects on MRI; 6) not initiated on disease-modifying therapy in the past six months, to avoid transient confounding effects on MRI of newly started therapy. Seven of the patients (54%) were receiving disease-modifying treatment at the time of the scan (Table 1). Six patients were receiving monotherapy with glatiramer acetate, and one patient was receiving beta-interferon and glatiramer acetate in combination. Eleven normal controls with a similar distribution of age and sex to the MS patients (Table 1) with no neurological symptoms or known neurological or major medical disorders were also included. T25FW data were not available in two patients. The current study was approved by our institutional review board and all subjects gave informed consent.

MRI acquisition

All patients underwent baseline brain MRI on the same scanner using the same scanning protocol. MRI was obtained on a 3 T unit (GE Signa, General Electric Healthcare, Milwaukee, WI) using a receive-only phased array head coil. Axial brain imaging included:

1. T2-prepared (3D) images, a novel pulse sequence [(Fig. 1) (Fautz et al., 2000)]: repetition time (TR) = 1500 ms, echo time (TE) = 30 and 90 ms, slice thickness = 2 mm (76 slices — no gap), matrix = 128 × 128, zero-filled to 256 × 256, flip angle = 90°, pixel size = 0.938 × 0.938 mm, number of signal averages = 1, acquisition time = 8 min. We obtained two image sets covering the whole brain — one for each echo time. The T2 prepared sequence was originally motivated by the desire to quantify excessive brain iron in patients with MS (Bakshi et al., 2008). Because iron containing ferritin affects T2 in a way that depends on the echo spacing, we wanted to obtain spin-echo, not fast spin-echo (FSE) contrast. However, spin-echo imaging of the whole brain is slow and less sensitive than FSE, so we used an FSE readout for the acquisition but with a spin-echo preparation as described in Fautz et al. (2000). After the spin-echo preparation, the entire slice encodes were performed in a centric ordered FSE acquisition. During the next TRs, the sequence was repeated with a different echo time of the preparation. The FSE readout was maintained the same for both TE images. Then the entire sequence was repeated with the *y* phase encode changed for the next acquisition. Our group has previously published a comparison of spin-echo prepared FSE T2 measurements and CSE T2 measurements in phantoms (de Bazelaire et al., 2004).
2. Fast fluid-attenuated inversion-recovery (FLAIR): TR = 9000 ms, TE = 151 ms, TI = 2250 ms, slice thickness = 2 mm (70 slices - no gap), matrix size = 256 × 256, pixel size = 0.976 × 0.976 mm, acquisition time = 9 minutes, number of signal averages = 1.
3. 3-D Spoiled Gradient Recalled (SPGR): TR = 7.9 ms, TE = 3.14 ms, flip angle = 15^0, slice thickness = 1.5 mm (124 slices no gap), matrix size = 256 × 256 × 124, pixel size = 0.938 × 0.938 × 1.5 mm, acquisition time = 7.5 minutes, number of signal averages = 1.

Data Analysis

MRI analysis was performed using the *Jim* software package (Version 4.0, Xinapse Systems, Northants, UK, http://www.xinapse.com).

Whole brain R2 maps

Whole brain R2 maps (Figure 2) were generated by using a least-squares fitting procedure, fitting the expression M=M0*exp(−TE*R2) (Whittall and MacKay, 1989;Press et al., 1992;Lawson and Hanson, 1974) from the two T2-weighted images (M0 = initial transverse magnetization; TE = echo time; R2 = 1/T2). In the present study, we chose to generate R2 rather than T2 maps because of the ability of R2 maps to show iron deposition as hyperintense areas, aiding clinical detection in relation to normal tissue. We expect to report in subsequent publications the exploration of gray matter iron deposition in MS using the R2-mapping method.

Whole brain NAWM R2 histograms

First, two of the source images, FLAIR and SPGR, were registered to their respective R2 map using a rigid registration algorithm in the Jim software package (translational and rotational only). Hyperintense lesions were segmented from the registered FLAIR images using a semiautomated edge-finding tool with manual corrections applied as needed (Figs. 3A, B) (Cader et al., 2006). A semiautomated masking tool was used to remove (mask) extracranial tissue on the registered SPGR images (Fig. 3) and then white matter was segmented from gray matter and CSF using an automated method based on intensity thresholding (Fig. 3). R2 maps containing only NAWM were then generated by masking the WM-only images from the SPGR

with the lesion masks from the FLAIR images (Figs. 3, 4). Global histograms from the NAWM R2 maps were generated with a bin width of 1 s^{-1} (Fig. 5), and the following histogram metrics were derived: peak height, peak position, and mean R2 (Fig. 2). The NAWM histogram in each individual was normalized by dividing each histogram count by the total number of pixels included to account for differences in mask size (intrasubject normalization). Whole brain NAWM R2 histogram data were not available for one control due to gross misclassification errors in the white matter segmentation process.

Regional brain white matter R2

Regions-of-interest (ROIs) were placed on non-binned floating point NAWM R2 maps to obtain mean R2 of selected regions. The regional NAWM areas, selected because of their large size to minimize partial volume effects and ease of identification were the frontal lobe, parietal lobe, and callosal splenium and genu (Fig. 4). Circular ROIs that were 5 mm in diameter, containing ~ 23 pixels were chosen (Bakshi et al., 2002). The 5 mm diameter was chosen so that the ROIs could be of uniform shape and size for all white matter areas, while fitting easily within the genu and splenium of the corpus callosum for all subjects, avoiding CSF. Ideally, the ROI size would be chosen to be as large as possible to minimize the standard deviation of the values, but this was limited by the smallest region of WM. Two ROIs (right and left) were drawn for the frontal lobe and parietal lobe white matter in the axial slice that represented the cranio-caudal midpoint of the lateral ventricles. The right and left ROI data were combined to form one set of data (45 pixels) for each of the frontal and parietal white matter areas. One ROI (23 pixels) was placed in the callosal splenium and genu using a sagittal view to aid accurate location. Caution was taken to ensure that the ROIs were placed in NAWM by avoiding MS lesions, gray matter, or CSF-containing spaces.

White matter volume

We derived two volumetric measures from the SPGR images to infer the extent of white matter atrophy using the segmentation procedures described above: 1) whole brain white matter volume and 2) whole brain NAWM volume. For the latter, the resulting images (Fig. 3) contained only the white matter compartment exclusive of areas (lesions) that were hyperintense on FLAIR images. Furthermore, for intrasubject normalization of the white matter volume, we divided these absolute volumes by the intracranial volume (ICV) to develop a whole brain white matter and whole brain NAWM fraction for each subject. The use of fractional data to assess brain atrophy was based on previous studies ([Bermel et al., 2003] and [Houtchens et al., 2007]). The ICV was determined from the SPGR images after masking of the extracranial tissue (Fig. 3). Whole brain white matter and whole brain NAWM volume fraction data were not available for one control due to misclassification errors in white matter segmentation process.

Reliability of MRI measurements

Variability was expressed as the mean coefficient of variation [COV = {(standard deviation divided by the mean) × 100%}]. The intra-rater COV in two MS patients and three healthy volunteers was estimated. The mean intra-rater COV was 0.46% (range: 0.02–1.22%) for R2 peak height, 0.00% (range: 0.00–0.00%) for R2 peak position, and 0.08% (range: 0.00–0.24%) for mean whole brain NAWM R2. The mean intra-rater COV was 1.32% (range: 0.18–2.35%) for frontal, 1.64% (range: 0.41–4.97%) for parietal, 2.31% (range: 0.32–7.77%) for callosal splenium and 1.75% (range: 0.27–3.87%) for callosal genu white matter areas R2.

Statistical analysis

Group differences between patients with MS and normal subjects in their demographic and MRI measures were evaluated using SAS® software v 9.1 of the SAS system for Windows

(SAS Institute Inc, Cary, NC). Group comparisons for age, mean R2, R2 histogram peak height and volumetric measures, were performed using a Wilcoxon-test and for sex and R2 histogram peak position using Fisher's exact test. Fisher's exact test was used for peak position because all patients' global WM data had values of either 15 or 16 s^{-1} for this measurement, due to the binning procedure. In addition, the 95% confidence intervals (CIs) for each group difference were determined to demonstrate the magnitude of the differences. Because age and sex could affect R2 and brain volume, these variables were also controlled for using rank ANCOVA (Stokes et al., 2000). Spearman correlation coefficient assessed the associations among MRI and clinical data. A *p*-value less than 0.05 was considered statistically significant in this exploratory study.

Results

Group comparisons: whole brain white matter R2

Whole brain NAWM R2 histogram results in patients with MS vs. normal controls are shown in Table 2 and Fig. 5. Mean R2 was significantly lower (indicating T2 prolongation) in patients with MS (15.46 ± 0.47 s^{-1}) than in normal controls (16.12 ± 0.20 s^{-1}) ($p = 0.00047$, 95% CI for group difference: −1.08, −0.29). Similarly, R2 peak position was significantly lower in patients with MS (15.54 ± 0.52 s^{-1}; 6/13 patients had 15 s^{-1}) than in normal controls (16.00 ± 0.00 s^{-1}; 0/10 had 15 s^{-1}) ($p = 0.019$, 95% CI for odds ratio: 0, 0.86). However, R2 peak height did not differ ($p = 0.93$, 95% CI: −0.02, 0.02). These results were unchanged after controlling for age and sex (data not shown).

Group comparisons: regional brain white matter R2

As shown in Table 3, in frontal white matter, significantly lower mean R2 was seen in patients with MS (mean R2 = 15.63 ± 0.80 s^{-1}) than in normal controls (mean R2 = 17.01 ± 0.59 s^{-1}) ($p = 0.00015$, 95% CI: −1.97, −0.57). In the parietal white matter, significantly lower mean R2 was observed in MS (mean R2 = 13.95 ± 0.75 s^{-1}) vs. controls (mean R2 = 14.53 ± 0.34 s^{-1}) ($p = 0.0069$, 95% CI: −1.05, −0.24). While mean R2 in the callosal genu was significantly lower in MS (mean R2 = 16.75 ± 1.78 s^{-1}) vs. controls (mean R2 = 18.60 ± 0.56 s^{-1}) ($p = 0.0019$, 95% CI: −2.84, −0.58), in the splenium, mean R2 did not differ ($p = 0.079$, 95% CI: −1.90, 0.043). These results were unchanged after controlling for age and sex (data not shown).

Group comparisons: whole brain white matter volume

Whole brain white matter and NAWM volume fractions did not differ significantly (all $p > 0.1$) between patients with MS and normal controls (Table 4), although a trend toward decreased whole brain NAWM fraction ($p = 0.078$) was observed when regression modeling was adjusted for age and sex in patients with MS (data not shown).

MRI–clinical correlations in the MS group

Correlations between whole brain NAWM R2 metrics and clinical measures (EDSS, T25FW and disease duration) were all non-significant ($p > 0.21$). Similarly, whole brain white matter and NAWM volume fractions were unrelated to EDSS and T25FW ($p > 0.32$). Only whole brain NAWM volume fraction showed a significant ($r = -0.62$; $p = 0.03$) inverse correlation with disease duration.

MRI–MRI correlations in the MS group

To test whether the severity of R2 reduction in the whole brain NAWM was associated with white matter atrophy, R2 metrics were related to whole brain white matter and NAWM volume fractions (Table 5). We found no significant correlation ($p > 0.25$) between R2 metrics and the whole brain white matter and NAWM volume fractions.

Post-hoc analysis

We performed a post-hoc analysis of the data after removing from the MS group the two patients with a primary ($n = 1$) or secondary ($n = 1$) progressive disease course, allowing us to examine the findings in the RRMS patients and determine if these differed from the overall cohort. The results were similar to what was seen in the whole MS group when examining MS vs. controls and correlations within the MS group (data not shown). Only the global NAWM R2 peak position that had shown a statistically significant difference between all MS patients ($n = 13$) and normal controls failed to show a significant difference between RRMS patients ($n = 11$) and normal controls ($p = 0.09$).

Discussion

In the present pilot study, we examined the ability of a novel pulse sequence applied at 3 T to derive T2 relaxation maps for the detection of diffuse occult damage in the white matter of patients with MS. The major finding of this study was that 3 T MRI histogram-based T2 measurements were able to detect microstructural changes characterized by T2 prolongation in NAWM in patients with MS at both the global and regional level. Such areas of damage did not manifest as overt lesions even though imaging was conducted at 3 T, yet were affected nonetheless by the disease as indicated by T2 prolongation. T2 measurements showed higher sensitivity in differentiating MS and normal control groups than did assessments of white matter atrophy.

Several comments are in order regarding how our study extends previous observations related to assessment of T2 relaxometry changes in NAWM in patients with MS. We applied a novel 3D FSE pulse sequence to quantify T2, which was based on a previously developed 2D pulse sequence (Fautz et al., 2000). Our pulse sequence had the unique advantage of providing high resolution images with whole brain coverage in a clinically feasible scan time. The multiple slice encodes used in 3D FSE have similar benefits to averaging of 2D images for improving SNR. In contrast, previous studies have employed T2 relaxometry calculations in patients with MS using pulse sequences that had limited brain coverage and longer scan times ([Stevenson et al., 2000], [Whittall et al., 2002], [Laule et al., 2004], [Laule et al., 2007], [Oh et al., 2007] and [Du et al., 2007]).

Another difference between our study and previous MS-related T2 relaxometry studies is the number of echoes employed to derive T2 values. Previous studies have relied on multi-echo rather than a two-echo approach. There are tradeoffs inherent in designing the scanning technique used to measure T2. With multi-echo studies, for example the use of 12 echoes (Oh et al., 2007), 32 echoes ([Laule et al., 2004] and [Whittall et al., 2002]) and 48 echoes (Laule et al., 2007), one can boost accuracy and generally more easily distinguish the subcomponents of the decay curve such as the short T2 component ([Whittall et al., 2002], [Laule et al., 2004] and [Oh et al., 2007]). However, this approach is limited by longer scan times, reduced brain coverage, difficulty performing multi-slice acquisitions, and incompatibility with 3D FSE. In addition, difficulties with applying the appropriate RF pulses may lead to artifactual variation over the field of view in measured T2.

Our study takes advantage of the notion that T2 quantification can be accurately performed using two echoes ([Breger et al., 1989] and [Smith et al., 2008]), as has been demonstrated to be effective in characterizing a variety of neurologic disorders such as epilepsy (Briellmann et al., 2004), Alzheimer's disease (Schenck et al., 2006) and leukodystrophy (Melhem et al., 2001). With this two-echo technique, a difference in echo times of approximately the T2 of the target tissue gives the highest precision in the measured R2. We showed a whole brain mean white matter R2 of ~ 16 s^{-1}, corresponding to a T2 of 62.5 ms; while the difference in echo times for our sequence was 60 ms, which is close to optimum. However, there are several

possible arguments against the use of two-echo T2 measurements (Whittall et al., 1999). The contribution of partial volume from CSF has been raised as a concern; but this is primarily a problem for gray matter, not white matter as studied here. Another argument is the multi-exponential character of white matter relaxation. At our echo times of 30 and 90 ms, the contribution of the short T2 component is very small, less than approximately 2% in the 30 TE image and negligible in the 90 TE image. Based on the simulation of Whittall et al. (1999), TE's of 30 and 90 ms would lead to 2 or 3 ms of T2 underestimation of the long T2 component. Interestingly, the simulation values for 1.5 T T2 of white matter using 30 and 90 ms TE are very similar to the previously reported mean T2s (Whittall et al., 2002). In addition, it is worth noting that our two-echo measurement produced a lower SD of T2 measurement than that of Whittall et al. (1999).

While FSE sequences can be used to generate T2-weighted contrast, there are potential errors associated when they are used for T2 quantification ([Majumdar et al., 1986a], [Majumdar et al., 1986b] and [Crawley and Henkelman, 1987]). Hence, we used a novel T2 sequence that is better described as a T2 prepared sequence which uses an FSE readout for the acquisition but with a spin-echo preparation to generate the desired contrast. With this sequence, we obtained two image sets covering the whole brain separately – one for each echo time – to create relaxation rate maps. Thus, by separating the imaging from the T2 contrast preparation we sought to avoid the limitations observed with multi-slice T2 that is vulnerable to slice interactions and a strong dependence on refocusing pulse amplitude and shape ([Majumdar et al., 1986a], [Majumdar et al., 1986b] and [Crawley and Henkelman, 1987]). A related approach has been used by Oh et al. (2007), to avoid problems from multiple echo T2 quantification, though they focused on the short T2 component and used multi-slice spiral instead of 3D FSE for acquisition. It should be emphasized that while 8 min is relatively long for a clinical sequence, for clinical research this approach may be a practical way to obtain T2 data in these patients. By using thicker slices (~ 3 mm) with an even shorter scanning time (~ 4 min), this approach may have potential for clinical research studies, or even routine clinical care in the future.

Relaxometry studies of patients with MS have shown promise in their ability to detect diffuse damage in areas of the brain and spinal cord (Neema et al., 2007a). In particular, the T2 relaxometry technique, based on transverse relaxation time mapping, can detect damage in NAWM that escapes detection by conventional MRI lesion measures ([Miller et al., 1989], [Laule et al., 2004] and [Whittall et al., 2002]). NAWM damage in patients with MS is characterized by a range of pathological changes of varying severity, such as demyelination, gliosis, inflammation, axonal injury, and axonal loss. Each of these would be expected to contribute to the T2 prolongation observed in our study (Bakshi et al., 2008). Very few previous studies have used high-field MRI to investigate T2 changes in NAWM, and these studies have focused on analysis of the short T2 component of the T2 decay curve, which is thought to represent water trapped between myelin bilayers (myelin water fraction — MWF) ([Oh et al., 2007] and [Du et al., 2007]). Reduced MWF, attributed to loss of myelin, has been described in NAWM ([Whittall et al., 2002], [Laule et al., 2004], [Oh et al., 2007] and [Du et al., 2007]). The short T2 component, although apparently specific for myelination, may not effectively assess other aspects of damage in the white matter, such as axonal loss, gliosis, and inflammation. The T2 measurements in the present study may thus have greater sensitivity, since it incorporates the intermediate component of T2, a marker of intra- and extracellular water ([Laule et al., 2007], [Grenier et al., 2002] and [Whittall et al., 2002]). Because of its long echo train, our strategy is incapable of imaging the short T2 component. Instead we have focused on the longer T2 components, which can generally be characterized by a single-exponential decay in the absence of significant partial volume averaging.

As expected from previous imaging studies (Neema et al., 2007b), we showed that the regional and global NAWM was abnormal in patients with MS. This is also in accord with other NAWM studies performed at 3 T using advanced measures such as MRS (Srinivasan et al., 2005), T1 relaxometry (Parry et al., 2003) and DTI (Ceccarelli et al., 2007). Regional analysis indicated that damage in the NAWM was widespread, involving frontal, parietal, and callosal areas. The callosal genu and anterior frontal white matter were particularly affected by T2 prolongation. The implication of the observed regional effect is unclear and requires confirmation in a larger study. Our findings are in agreement with data showing a substantial loss of axonal fibers in the corpus callosum in patients with MS (Evangelou et al., 2000). In the present study, the lack of association between T2 measures and clinical status should be interpreted with caution as the small sample size and cross-sectional study design may have limited the ability to show MRI-clinical correlations. Alternatively, other clinical measures such as cognitive function or fatigue, which may have been related to diffuse white matter integrity ([Zivadinov et al., 2001] and [Tartaglia et al., 2004]), were not assessed in our study. We also did not find a relationship between white matter atrophy measures and clinical measures of disability in agreement with previous studies (Bermel and Bakshi, 2006). However, overall, this study was likely underpowered to be able to demonstrate clinical–MRI correlations.

In addition, there was a lack of correlation observed between T2 measurements and white matter volume fractions. The severity of R2 reduction was not associated with reductions in the normalized WM volume fractions suggesting that T2 increases were not associated with white matter atrophy. In the present sample, we did not find a significant difference in white matter volumes in patients with MS and normal controls (i.e. no evidence of white matter atrophy). Another consideration is the differential effects of the disease process causing substantial gray matter but only minimal white matter atrophy ([Dalton et al., 2004], [Sanfilipo et al., 2005], [Valsasina et al., 2005] and [Bermel and Bakshi, 2006]). Taken together these findings suggest that T2 changes in NAWM may be more sensitive to disease effects than measures of white matter atrophy. One possible explanation for this differential sensitivity is that inflammatory demyelination and gliosis, reflected in T2 prolongation, may precede the onset of axonal loss and tissue degeneration, reflected in loss of brain bulk (Simon et al., 2000). Other factors that may have contributed to our results include tissue changes that could mask the atrophy of white matter such as edema or lymphocytic infiltration (Dalton et al., 2004). Our findings may also be related to the stage of disease and small number of patients in our sample; therefore the pathologic explanation and interpretation should be considered speculative.

There is a growing interest in the routine clinical use of 3 T MRI in the diagnostic and longitudinal evaluation of patients with MS (Bakshi et al., 2008). Despite the ability of MRI at 3 T to detect overt lesions with greater sensitivity than at 1.5 T ([Sicotte et al., 2003], [Wattjes et al., 2006] and [Bachmann et al., 2006]: Stankiewicz et al., 2008), our study indicates that there remain areas of hidden damage outside of detectable focal lesions, even on a 3 T platform. The improved SNR (Schick, 2005) at 3 T potentially allowed us to capture images with relatively small voxel sizes serving to minimize variance in R2 measurements. It is important to have markers of neurodegenerative changes in MS that are sensitive and reproducible. The high degree of intra-rater reproducibility and sensitivity supports the feasibility of the proposed method. Our findings have the potential implication of introducing a 3 Minnerop et al., 2007), rather than ROI approaches to study spatial distribution of damage. However, the modest number of subjects included in this study did not permit this approach, and we plan to pursue voxel-based relaxometry analyses of R2 maps in the future with a larger cohort. New techniques of parallel imaging, not applied in the present study, may permit faster acquisition of 3D volumes. Such a capability might make possible improved spatial resolution, a greater number of echo times, and possibly reduced scan time.

The multicomponent T2 relaxometry analysis we applied is not specific for the underlying pathology (Neema et al., 2007a) and its sensitivity to damage in NAWM might be reduced because of an offsetting effect of T2 shortening caused by, for example, deposition of iron or other paramagnetic substances ([Craelius et al., 1982] and [Janardhan et al., 2007]). The clinical relevance and the longitudinal sensitivity should be assessed in future studies to extend our findings. Future work should compare whether this technique has a better clinical correlation and predictive value for clinical outcome than other MRI measures, such as spectroscopy, diffusion tensor and magnetization transfer (MT) MRI. In this context it is interesting to note that strong correlations between T2 relaxation time and MT ratio have been reported in the dirty white matter but not NAWM in the brains of patients with MS at 1.5 T (Papanikolaou et al., 2004). Thus, future studies should compare these methods at 3 T to explore their relative reliability, sensitivity and validity and to determine to what extent one technique obviates the need for the other in the study of white matter integrity.

In summary, this pilot study using a 3 T MRI scanner shows that hidden damage is present in the brain white matter of patients with MS that escapes detection as overt focal lesions. We have shown that an FSE 3D T2 prepared sequence can derive T2 relaxometry in a clinically acceptable scan time that is sensitive to this diffuse occult pathology, characterized by T2 prolongation in NAWM in patients with MS.

Acknowledgments

This work was supported by research grants from the National Institutes of Health (NIH-NINDS K23 NS42379-01 and R01 NS055083-01) and National Multiple Sclerosis Society (RG3705A1; RG3798A2; RG4032A1/1). We thank Ms. Sophie Tamm for her assistance with manuscript preparations.

References

Armspach JP, Gounot D, Rumbach L, Chambron J. In vivo determination of multiexponential T2 relaxation in the brain of patients with multiple sclerosis. Magn Reson Imaging 1991;9:107–113. [PubMed: 2056848]

Bachmann R, Reilmann R, Schwindt W, Kugel H, Heindel W, Krämer S. FLAIR imaging for multiple sclerosis: a comparative MR study at 1.5 and 3.0 Tesla. Eur Radiol 2006;16:915–921. [PubMed: 16365731]

Bakshi R, Benedict RH, Bermel RA, Caruthers SD, Puli SR, Tjoa CW, Fabiano AJ, Jacobs L. T2 hypointensity in the deep gray matter of patients with multiple sclerosis: a quantitative magnetic resonance imaging study. Arch Neurol 2002;59:62–68. [PubMed: 11790232]

Bakshi R, Minagar A, Jaisani Z, Wolinsky JS. Imaging of multiple sclerosis: role in neurotherapeutics. NeuroRx 2005;2:277–303. [PubMed: 15897951]

Bakshi R, Thompson AJ, Rocca MA, Pelletier D, Dousset V, Barkhof F, Inglese M, Guttmann CR, Horsfield MA, Filippi M. MRI in multiple sclerosis: current status and future prospects. Lancet Neurol 2008;7:615–625. [PubMed: 18565455]

Barbosa S, Blumhardt LD, Roberts N, Lock T, Edwards RH. Magnetic resonance relaxation time mapping in multiple sclerosis: normal appearing white matter and the “invisible” lesion load. Magn Reson Imaging 1994;12:33–42. [PubMed: 8295506]

Bermel RA, Bakshi R. The measurement and clinical relevance of brain atrophy in multiple sclerosis. Lancet Neurol 2006;5:158–170. [PubMed: 16426992]

Bermel RA, Sharma J, Tjoa CW, Puli SR, Bakshi R. A semiautomated measure of whole-brain atrophy in multiple sclerosis. J Neurol Sci 2003;208:57–65. [PubMed: 12639726]

Breger RK, Rimm AA, Fischer ME, Papke RA, Haughton VM. T1 and T2 measurements on a 1.5-T commercial MR imager. Radiology 1989;171:273–276. [PubMed: 2928538]

Briellmann RS, Syngeniotis A, Fleming S, Kalnins RM, Abbott DF, Jackson GD. Increased anterior temporal lobe T2 times in cases of hippocampal sclerosis: a multi-echo T2 relaxometry study at 3 T. AJNR Am J Neuroradiol 2004;25:389–394. [PubMed: 15037460]

Cader S, Cifelli A, Abu-Omar Y, Palace JJ, Matthews PM. Reduced brain functional reserve and altered functional connectivity in patients with multiple sclerosis. Brain 2006;129:527–537. [PubMed: 16251214]

Ceccarelli A, Rocca MA, Falini A, Tortorella P, Pagani E, Rodegher M, Comi G, Scotti G, Filippi M. Normal-appearing white and grey matter damage in MS. A volumetric and diffusion tensor MRI study at 3.0 Tesla. J Neurol 2007;254:513–518. [PubMed: 17401516]

Craelius W, Migdal MW, Luessenhop CP, Sugar A, Mihalakis I. Iron deposits surrounding multiple sclerosis plaques. Arch Pathol Lab Med 1982;106:397–399. [PubMed: 6896630]

Crawley AP, Henkelman RM. Errors in T2 estimation using multislice multiple-echo imaging. Magn Reson Med 1987;4:34–47. [PubMed: 3821477]

Dalton CM, Chard DT, Davies GR, Miszkiel KA, Altmann DR, Fernando K, Plant GT, Thompson AJ, Miller DH. Early development of multiple sclerosis is associated with progressive grey matter atrophy in patients presenting with clinically isolated syndromes. Brain 2004;127:1101–1107. [PubMed: 14998914]

de Bazelaire CM, Duhamel GD, Rofsky NM, Alsop DC. MR imaging relaxation times of abdominal and pelvic tissues measured in vivo at 3.0 T: preliminary results. Radiology 2004;230:652–659. [PubMed: 14990831]

Du YP, Chu R, Hwang D, Brown MS, Kleinschmidt-DeMasters BK, Singel D, Simon DH. Fast multislice mapping of the myelin water fraction using multicompartment analysis of T2* decay at 3 T: a preliminary postmortem study. Magn Reson Med 2007;58:570–865.

Evangelou N, Esiri MM, Smith S, Palace J, Matthews PM. Quantitative pathological evidence for axonal loss in normal appearing white matter in multiple sclerosis. Ann Neurol 2000;47:391–395. [PubMed: 10716264]

Fautz HP, Büchert M, Husstedt H, Laubenberger J, Hennig J. TSE sequences with spin-echo contrast. Magn Reson Med 2000;43:577–582. [PubMed: 10748433]

Gauthier SA, Glanz BI, Mandel M, Weiner HL. A model for the comprehensive investigation of a chronic autoimmune disease: the multiple sclerosis CLIMB study. Autoimmun Rev 2006;5:532–536. [PubMed: 17027888]

Grenier D, Pelletier D, Normandeau M, Newitt D, Nelson S, Goodkin DE, Majumdar S. T2 relaxation time histograms in multiple sclerosis. Magn Reson Imaging 2002;20:733–741. [PubMed: 12591569]

Houtchens MK, Benedict RH, Killiany R, Sharma J, Jaisani Z, Singh B, Weinstock-Guttman B, Guttmann CR, Bakshi R. Thalamic atrophy and cognition in multiple sclerosis. Neurology 2007;69:1213–1223. [PubMed: 17875909]

Janardhan V, Suri S, Bakshi R. Multiple sclerosis: hyperintense lesions in the brain on nonenhanced T1-weighted MR images evidenced as areas of T1 shortening. Radiology 2007;244:823–831. [PubMed: 17690319]

Kurtzke JF. Rating neurologic impairment in multiple sclerosis: an expanded disability status scale (EDSS). Neurology 1983;33:1444–1452. [PubMed: 6685237]

Laule C, Vavasour IM, Moore GR, Oger J, Li DK, Paty DW, MacKay AL. Water content and myelin water fraction in multiple sclerosis: a T2 relaxation study. J Neurol 2004;251:284–293. [PubMed: 15015007]

Laule C, Vavasour IM, Kolind SH, Traboulsee AL, Moore GR, Li DK, MacKay AL. Long T2 water in multiple sclerosis: what else can we learn from multi-echo T2 relaxation? J Neurol 2007;254:1579–1587. [PubMed: 17762945]

Lawson, CL.; Hanson, RJ. Solving Least Squares Problems. Prentice-Hall; Englewood Cliffs, NJ: 1974. p. 1-311.

Majumdar S, Orphanoudakis SC, Gmitro A, O'Donnell M, Gore JC. Errors in the measurements of T2 using multiple-echo MRI techniques. I. Effects of radiofrequency pulse imperfections. Magn Reson Med 1986;3:397–417. [PubMed: 3724419]

Majumdar S, Orphanoudakis SC, Gmitro A, O'Donnell M, Gore JC. Errors in the measurements of T2 using multiple-echo MRI techniques. II. Effects of static field inhomogeneity. Magn Reson Med 1986;3:562–574. [PubMed: 3747818]

Melhem ER, Gotwald TF, Itoh R, Zinreich SJ, Moser HW. T2 relaxation measurements in X-linked adrenoleukodystrophy performed using dual-echo fast fluid-attenuated inversion recovery MR imaging. AJNR Am J Neuroradiol 2001;22:773–776. [PubMed: 11290498]

Miller DH, Johnson G, Tofts PS, MacManus D, McDonald WI. Precise relaxation time measurements of normal-appearing white matter in inflammatory central nervous system disease. Magn Reson Med 1989;11:331–336. [PubMed: 2779420]

Minnerop M, Specht K, Ruhlmann J, Schimke N, Abele M, Weyer A, Wüllner U, Klockgether T. Voxel-based morphometry and voxel-based relaxometry in multiple system atrophy—a comparison between clinical subtypes and correlations with clinical parameters. NeuroImage 2007;36:1086–1095. [PubMed: 17512219]

Neema M, Stankiewicz J, Arora A, Dandamudi VS, Batt CE, Guss ZD, Al-Sabbagh A, Bakshi R. T1- and T2-based MRI measures of diffuse gray matter and white matter damage in patients with multiple sclerosis. J Neuroimaging 2007;17:16S–21S. [PubMed: 17425729]

Neema M, Stankiewicz J, Arora A, Guss ZD, Bakshi R. MRI in multiple sclerosis: what's inside the toolbox? Neurotherapeutics 2007;4:602–617. [PubMed: 17920541]

Oh J, Han ET, Lee MC, Nelson SJ, Pelletier D. Multislice brain myelin water fractions at 3 T in multiple sclerosis. J Neuroimaging 2007;17:156–163. [PubMed: 17441837]

Papanikolaou N, Papadaki E, Karampekios S, Spilioti M, Maris T, Prassopoulos P, Gourtsoyiannis N. T2 relaxation time analysis in patients with multiple sclerosis: correlation with magnetization transfer ratio. Eur Radiol 2004;14:115–122. [PubMed: 14600774]

Parry A, Clare S, Jenkinson M, Smith S, Palace J, Matthews PM. MRI brain T1 relaxation time changes in MS patients increase over time in both the white matter and the cortex. J Neuroimaging 2003;13:129–234.

Polman CH, Reingold SC, Edan G, Filippi M, Hartung HP, Kappos L, Lublin FD, Metz LM, McFarland HF, O'Connor PW, Sandberg-Wollheim M, Thompson AJ, Weinshenker BG, Wolinsky JS. Diagnostic criteria for multiple sclerosis: 2005 revisions to the "McDonald Criteria". Ann Neurol 2005;58:840–846. [PubMed: 16283615]

Press, W.; Teukolsky, S.; Vetterling, W.; Flannery, B. Numerical Recipes in C. 2. Cambridge University Press; Cambridge, UK: 1992.

Sanfilipo MP, Benedict RH, Sharma J, Weinstock-Guttman B, Bakshi R. The relationship between whole brain volume and disability in multiple sclerosis: a comparison of normalized gray vs. white matter with misclassification correction. NeuroImage 2005;26:1068–1077. [PubMed: 15961046]

Schenck JF, Zimmerman EA, Li Z, Adak S, Saha A, Tandon R, Fish KM, Belden C, Gillen RW, Barba A, Henderson DL, Neil W, O'Keefe T. High-field magnetic resonance imaging of brain iron in Alzheimer disease. Top Magn Reson Imaging 2006;17:41–50. [PubMed: 17179896]

Schick F. Whole-body MRI at high field: technical limits and clinical potential. Eur Radiol 2005;15:946–959. [PubMed: 15856252]

Sicotte NL, Voskuhl RR, Bouvier S, Klutch R, Cohen MS, Mazziotta JC. Comparison of multiple sclerosis lesions at 1.5 and 3.0 Tesla. Invest Radiol 2003;38:423–427. [PubMed: 12821856]

Simon JH, Kinkel RP, Jacobs L, Bub L, Simonian N. A Wallerian degeneration pattern in patients at risk for MS. Neurology 2000;54:1155–1160. [PubMed: 10720290]

Smith SA, Edden RA, Farrell JA, Barker PB, Van Zijl PC. Measurement of T1 and T2 in the cervical spinal cord at 3 Tesla. Magn Reson Med 2008;60:213–219. [PubMed: 18581383]

Srinivasan R, Sailasuta N, Hurd R, Nelson S, Pelletier D. Evidence of elevated glutamate in multiple sclerosis using magnetic resonance spectroscopy at 3 T. Brain 2005;128:1016–1025. [PubMed: 15758036]

Stankiewicz JM, Glanz B, Healy BC, Arora A, Neema M, Benedict RHB, Guss ZD, Buckle GJ, Houtchens MK, Khoury S, Weiner HL, Guttmann CRG, Bakshi R. Brain MRI lesion volume correlates with physical disability and cognitive impairment in multiple sclerosis: comparison of 1.5 T and 3 T. Neurology 2008;70:A473.

Stevenson VL, Parker GJ, Barker GJ, Birnie K, Tofts PS, Miller DH, Thompson AJ. Variations in T1 and T2 relaxation times of normal appearing white matter and lesions in multiple sclerosis. J Neurol Sci 2000;178:81–87. [PubMed: 11018698]

Stokes, ME.; Davis, CS.; Koch, GG. Categorical Data Analysis Using the SAS System. 2. SAS Institute Inc; Cary, NC: 2000.

Tartaglia MC, Narayanan S, Francis SJ, Santos AC, De Stefano N, Lapierre Y, Arnold DL. The relationship between diffuse axonal damage and fatigue in multiple sclerosis. Arch Neurol 2004;61:201–207. [PubMed: 14967766]

Valsasina P, Benedetti B, Rovaris M, Sormani MP, Comi G, Filippi M. Evidence for progressive gray matter loss in patients with relapsing-remitting MS. Neurology 2005;65:1126–1128. [PubMed: 16217074]

Wattjes MP, Lutterbey GG, Harzheim M, Gieseke J, Träber F, Klotz L, Klockgether T, Schild HH. Higher sensitivity in the detection of inflammatory brain lesions in patients with clinically isolated syndromes suggestive of multiple sclerosis using high field MRI: an intraindividual comparison of 1.5 T with 3.0 T. Eur Radiol 2006;16:2067–2073. [PubMed: 16649033]

Whittall KP, MacKay AL. Quantitative interpretation of NMR relaxation data. J Magn Reson 1989;84:64–71.

Whittall KP, MacKay AL, Li DK. Are mono-exponential fits to a few echoes sufficient to determine T2 relaxation for in vivo human brain? Magn Reson Med 1999;41:1255–1257. [PubMed: 10371459]

Whittall KP, MacKay AL, Li DK, Vavasour IM, Jones CK, Paty DW. Normal-appearing white matter in multiple sclerosis has heterogeneous, diffusely prolonged T(2). Magn Reson Med 2002;47:403–408. [PubMed: 11810687]

Zivadinov R, De Masi R, Nasuelli D, Bragadin LM, Ukmar M, Pozzi-Mucelli RS, Grop A, Cazzato G, Zorzon M. MRI techniques and cognitive impairment in the early phase of relapsing-remitting multiple sclerosis. Neuroradiology 2001;43:272–278. [PubMed: 11338408]

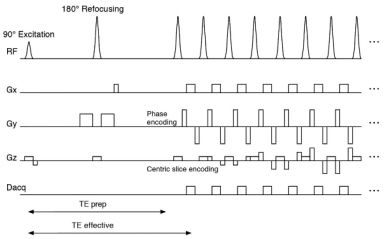

Fig. 1.

Pulse sequence used for T2 relaxometry. A spin-echo preparation of duration TEprep is applied prior to a fast spin echo acquisition. The sum of TEprep and the additional time to the first data acquisition provide the effective TE of the sequence. In our acquisition, two images with different effective TE's were acquired by changing TEprep. Data was acquired with a specific phase encoding amplitude for the first effective TE and then repeated with the second effective TE. The phase encoding amplitude was then incremented and the pattern was repeated until the entire image is encoded.

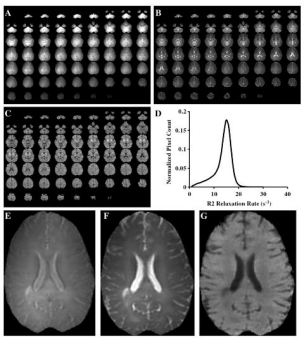

Fig. 2.

Source T2 images and generation of whole brain R2 maps from a patient with MS. The upper row shows the axial T2 source images [TE = 30 ms (A) and TE = 90 ms (B)]. The R2 maps (middle-left; C) are then calculated on a pixel-by-pixel basis from the source images using a least-squares fitting algorithm. A whole brain R2 histogram (D) can then be derived from all nonzero pixels in the R2 map. Note – The histogram is for illustrative purpose only – the R2 histograms generated in the present study were from lesion-removed images of normal-appearing white matter — see Methods section and Figs. 3, 4. A representative mid-ventricular slice from figures A–C is enlarged in figures E–G.

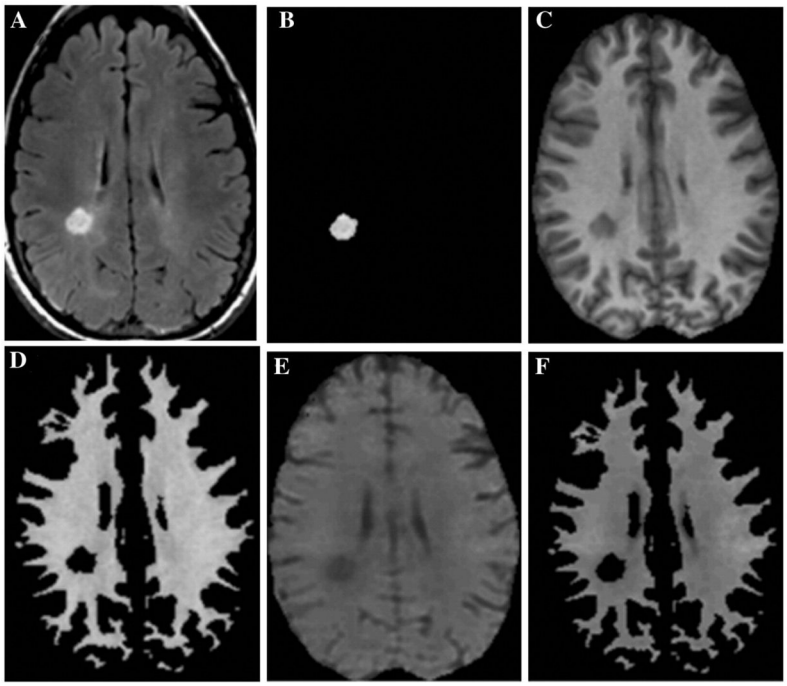

Fig. 3.

Representative slices from a patient with MS showing processing to develop R2 maps of the cerebral normal-appearing white matter (NAWM). (A) raw FLAIR (B) segmented FLAIR lesion-only image. (C) raw SPGR image after removal of extracranial tissue (masking) (D) segmented white matter-only SPGR image. (E) raw R2 map after masking (F) segmented NAWM R2 map (with lesions, gray matter, and CSF removed) obtained from B, D and E.

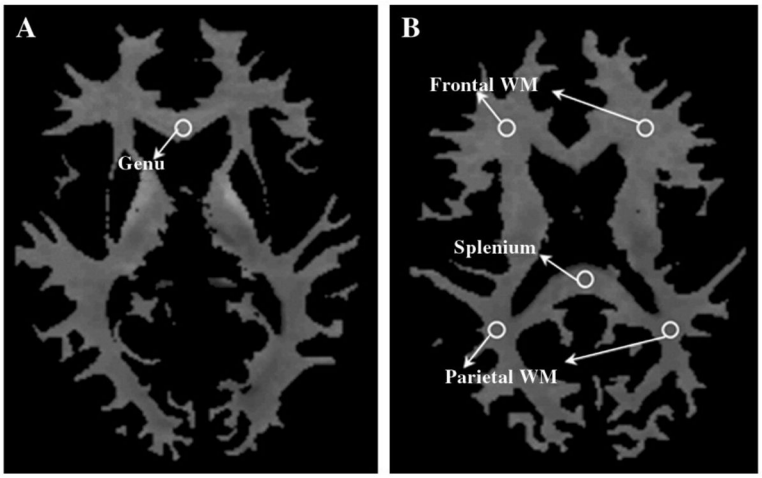

Fig. 4.

Representative slices from a patient with MS showing the standardized regions-of-interest (ROIs) template used to evaluate regional normal-appearing white matter (NAWM). Segmented NAWM R2 masks are shown (with lesions, gray matter, and CSF removed) on which circular 5 mm ROIs were placed by an experience observer. Two ROIs were drawn (right and left) in the frontal lobe and parietal lobe white matter (WM) at the mid-ventricular level while one ROI was drawn in each of the callosal genu (A) and splenium (B). See Methods section for more details.

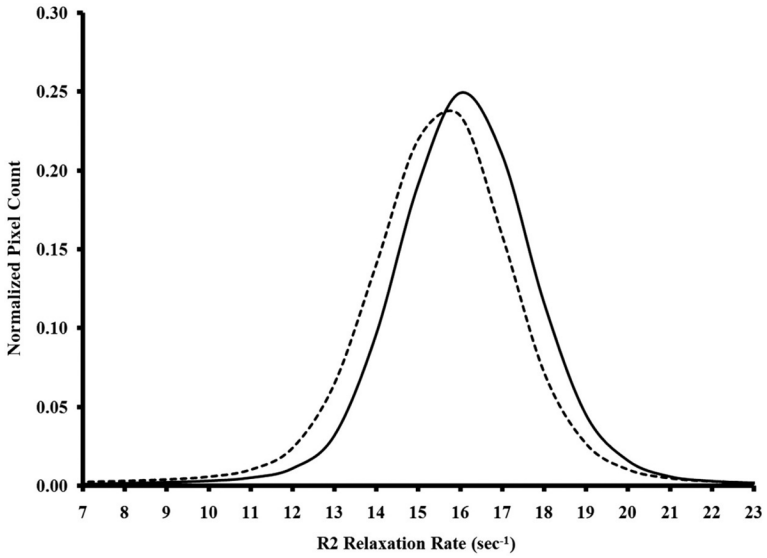

Fig. 5.

Whole brain normal-appearing white matter (NAWM) histograms for combined normal controls (solid black line) and patients with MS (dashed line). Note a left shift of the MS curve indicating R2 shortening (i.e. T2 prolongation) in the NAWM in the MS group.

Table 1

Demographic and clinical characteristics.

	Normal controls	Multiple sclerosis
Subjects	11	13
Men/women[a]	6/5	6/7
Age (years)[a]	42.1 ± 5.7 (33–51)	42.5 ± 5.4 (33–51)
Disease duration (years from first symptoms)	–	9.0 ± 6.4 (1–22)
Disease course:		
Relapsing-remitting	–	11
Secondary progressive	–	1
Primary progressive	–	1
Expanded Disability Status Scale score	–	2.5 ± 1.7 (1.0–6.5)
Timed 25-foot walk	–	5.1 ± 1.1 (3.8–8)
Patients on disease-modifying therapy[b]	–	7 (54%)[b]

Key: Values in table are mean ± SD (range).

[a]No significant group differences when comparing normal controls and patients.

[b]6 patients on glatiramer acetate and 1 patient on combined glatiramer acetate and interferon.

Table 2

Whole brain normal-appearing white matter R2 histogram results.

Whole brain NAWM	NL	MS	*p*-value (NL vs. MS)	Point estimate (95% confidence interval)
Mean relaxation rate (s^{-1})	16.12 ± 0.20	15.46 ± 0.47	0.00047	−0.61 (−1.08, −0.29)
Peak position	16.00 ± 0.00	15.54 ± 0.52	0.019	0 (0, 0.86)
Peak height	0.25 ± 0.02	0.25 ± 0.02	0.93	0.001 (- 0.02, 0.02)

Key: values in table are mean ± SD; NAWM = normal-appearing white matter; NL = normal controls; MS = multiple sclerosis.

Table 3

Regional brain normal-appearing white matter R2.

NAWM structure	NL	MS	*p*-value (NL vs. MS)	Point estimate (95% confidence interval)
Frontal	17.01 ± 0.59	15.63 ± 0.80	0.00015	−1.46 (−1.97, −0.57)
Parietal	14.53 ± 0.34	13.95 ± 0.75	0.0069	−0.66 (−1.05, −0.24)
Callosal genu	18.60 ± 0.56	16.75 ± 1.78	0.0019	−1.56 (−2.84, −0.58)
Callosal splenium	15.77 ± 1.04	14.87 ± 1.08	0.079	−0.66 (−1.90, 0.043)

Key: values in table are R2 (s^{-1}) mean ± SD; NAWM = normal-appearing white matter; NL = normal controls; MS = multiple sclerosis.

Table 4

White matter atrophy measures.

	NL	MS	*p*-value (NL vs. MS)
Whole brain NAWM volume fraction	0.3427 ± 0.0218	0.3268 ± 0.0178	0.12
Whole brain white matter volume fraction	0.3428 ± 0.0218	0.3331 ± 0.0161	0.23

Key: values in table are mean ± SD; NAWM = normal-appearing white matter; NL = normal controls; MS = multiple sclerosis.

Table 5

Correlations between R2 metrics and white matter atrophy measures in the MS group.

	Whole brain NAWM R2		
	Mean relaxation rate	**Peak position**	**Peak height**
	***r* (*p*)**	***r* (*p*)**	***r* (*p*)**
Whole brain NAWM volume fraction	−0.21 (0.48)	0.04 (0.89)	−0.21 (0.48)
Whole brain white matter volume fraction	−0.23 (0.46)	−0.08 (0.79)	−0.34 (0.25)

Key: NAWM = normal-appearing white matter.